Journal of Alloys and Compounds 509 (2011) 7591–7594

Contents lists available at ScienceDirect

Journal of Alloys and Compounds

journal homepage: www.elsevier.com/locate/jallcom

Ferroelectric and magnetic properties in high-pressure synthesized $BiFeO_3$ compound

L. Zhai[a], Y.G. Shi[b], J.L. Gao[a], S.L. Tang[a,*], Y.W. Du[a]

[a] Nanjing National Laboratory of Microstructures, Jiangsu Provincial Laboratory for Nanotechnology, Nanjing University, Nanjing 210093, China
[b] Department of Applied Physics, Nanjing University of Aeronautics and Astronautics, Nanjing 210016, China

ARTICLE INFO

Article history:
Received 16 February 2011
Received in revised form 5 April 2011
Accepted 6 April 2011
Available online 16 April 2011

PACS:
75.85.+t
77.80.−e
75.50.Ee

Keywords:
Multiferroic
$BiFeO_3$
High-pressure synthesis
Magnetization
Ferroelectricity

ABSTRACT

High-density polycrystalline $BiFeO_3$ compound was synthesized by high-pressure annealing. Measurements of crystal structure, magnetic, and ferroelectric properties were made on the sample. It was found that the sample was almost single phase with a distorted $R3c$ structure. The results of the X-ray photoelectron spectra demonstrate that the oxidation state of Fe in the sample is Fe^{3+}. The room-temperature field dependence of magnetization for $BiFeO_3$ exhibits a hysteretic behavior. The observed weak ferromagnetism could be ascribed to the lattice distortion induced by the high-pressure annealing. In addition, the local ferroelectric performance of the sample was studied by piezoresponse force microscopy.

1. Introduction

Multiferroic materials have attracted an ever-increasing attention in recent years due to the potential applications in sensors, data storage devices, transducers, etc. Among these multiferroic materials, $BiFeO_3$ is the most extensively studied material, because of its high ferroelectric Curie temperature $T_c \sim 1103$ K, and antiferromagnetic Néel temperature $T_N \sim 657$ K [1–4]. The magnetic structure of $BiFeO_3$ is antiferromagnetic with G-type ordering. This G-type antiferromagnetic is slightly modulated to a cycloidal spiral structure with a period of 62 nm length with [1 1 0] as the spiral propagation direction and spin rotation within (1 1 0), thereby producing a helimagnetic order and a vanishing net magnetization in the bulk at room temperature [5,6]. On the other hand, $BiFeO_3$ is metastable in air. The kinetics of phase formation in the Bi_2O_3–Fe_2O_3 system can easily lead to the appearance of unwanted phases, such as $Bi_2Fe_4O_9$ and $Bi_{25}FeO_{40}$[7]. In order to obtain single-phase $BiFeO_3$ polycrystalline ceramic with high resistivity, a series of method was developed in the past few years, such as solid state reaction method followed by leaching the impurity phase with dilute nitric acid [8], rapid liquid phase sintering [9] or conventional solid state reaction combined quenching process [10]. Recently, high-pressure annealing method has been proved to be an effective way to synthesize metastable phase Bi-based materials, such as, $BiMnO_3$[11], $BiCrO_3$[12] or $BiAlO_3$[13]. Therefore, it is interesting to investigate the structure and multiferroic properties of $BiFeO_3$ synthesized by the high-pressure annealing method. In the present work, a high-density polycrystalline $BiFeO_3$ ceramic was synthesized by high-pressure annealing method. Its crystal structure, magnetic and ferroelectric properties were reported.

2. Experiments

The high purity of Bi_2O_3 and Fe_2O_3 (*purity* ~ 99.999%) were weighed and stoichiometrically mixed in an agate mortar for 12 h using alcohol as a medium. This mixture was pressed into disk and precalcined at 750 °C for 3 h. The precursor mixture (about 1 g for a sample) was then calcined at 800 °C for 40 min at a pressure of 6 GPa by a hexahedral anvil high-pressure annealing apparatus. The details of the high-pressure annealing apparatus were described before [14]. After calcining, the samples were quickly cooled to room temperature, and the pressure was slowly released to the normal pressure.

The structure of $BiFeO_3$ was determined with X-ray diffraction data. XRD patterns were collected at room temperature using a Rigaku D/Max-gA diffractometer with Cu kα radiation ($\lambda = 1.54505$ Å). The data were analyzed by the Rietveld method using the General Structure Analysis System (GSAS) [15]. Oxidation of Fe was determined by X-ray photoelectron spectroscopy (XPS) (ESCALab MK-II). The fresh fracture surface of the samples was observed using scanning electron microscopy

---

* Corresponding author. Tel.: +86 25 83593817; fax: +86 25 83595535.
E-mail address: tangsl@nju.edu.cn (S.L. Tang).

0925-8388/$ – see front matter © 2011 Elsevier B.V. All rights reserved.
doi:10.1016/j.jallcom.2011.04.046

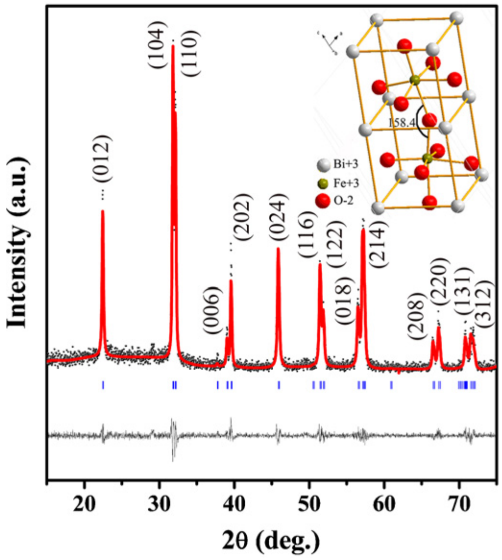

Fig. 1. Observed (circles), calculated (solid line) and difference (solid line at the bottom) XRD patterns for $BiFeO_3$ at room temperature. Bragg reflections are indicated by ticks. The inset shows the schematic of the crystal structure of $BiFeO_3$.

(SEM). Domain images were observed by the piezoelectric force microscopy (PFM) mode using a commercial atomic force microscope (Digital Instruments, NanoScope V, Veeco) equipped with a Pt/Ir coated Cr tip in PFM mode. The tip radius was less than 20 nm and a force constant of 4 N/m was use to study the piezoresponse of the regions without top electrodes. Domain visualization was performed under an applied ac voltage with the amplitude $V_{ac} = 5$ V and frequency $f = 50$ kHz. Magnetic properties were investigated using a superconducting quantum interference device (SQUID) magnetometer.

3. Results and discussion

It was found that calcining the starting mixtures before high-pressure annealing is helpful to obtain the $BiFeO_3$ phase. It is difficult to synthesize $BiFeO_3$ single phase by one-step annealing the starting materials, even at a wide range of annealing temperature from 800 to 1300 °C. However, $BiFeO_3$ with almost single phase can be easily formed by high-pressure annealing the calcined powders at a low temperature of 800 °C. The typical XRD patterns of the synthesized $BiFeO_3$ compound is shown in Fig. 1. Based on the XRD pattern, a simulation was carried out using rhombohedral lattice type with *R*3*c* space group. The simulation results and the differences between experiment and simulation are also shown in Fig. 1. The Rietveld refinements of crystal structure parameters are listed in Table 1. Compared with the structure of the $BiFeO_3$ synthesized under normal pressure [10,16], the atom positions, lattice parameters and interatomic distances show significant distortion. For clarity, the inset of Fig. 1 shows the schematic of the crystal structure of the sample. In contrast with the Fe–O–Fe angle 154.1° in $BiFeO_3$ single crystal [16], the corresponding angle in our sample is estimated to be 158.4°. Therefore, our sample possesses a distorted *R*3*c* crystal structure. The distortion should be ascribed to the effects of high-pressure annealing.

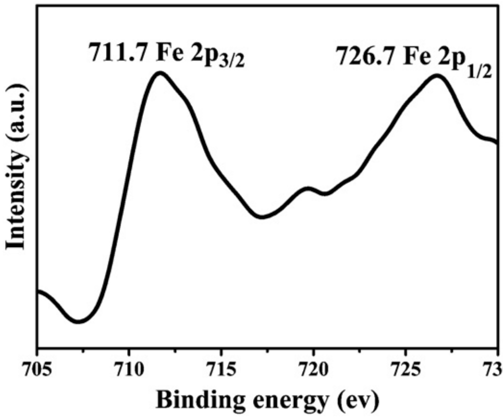

Fig. 2. X-ray photoelectron spectra of the Fe 2p lines for $BiFeO_3$.

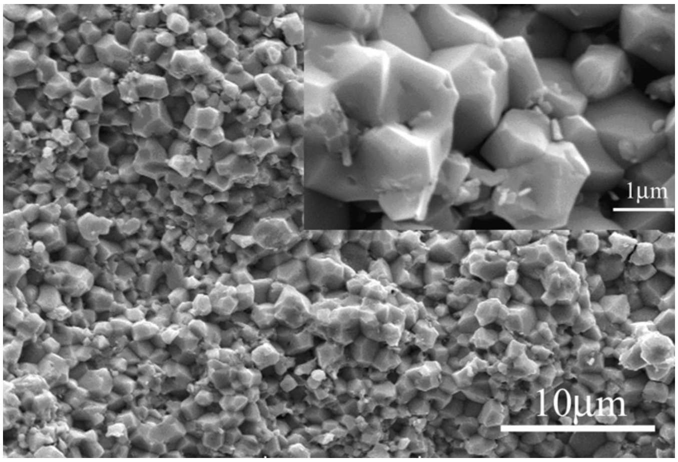

Fig. 3. SEM image of fracture surface for $BiFeO_3$.

In order to determine the valence states of Fe ions, XPS analysis was performed on the $BiFeO_3$ compound. Fig. 2 shows the Fe 2p spectra of the sample. The peaks near 711.7 eV and 726.7 eV are corresponding to Fe $2p_{3/2}$ and Fe $2p_{1/2}$, respectively, which are characteristic of Fe^{3+} ions [17]. Therefore, it can be deduced that the oxidation state of Fe ion should be Fe^{3+} but not Fe^{2+}.

Fig. 3 shows SEM image taken from fresh fracture surface for $BiFeO_3$. It can be seen that the ceramic was a dense one, without significant residual porosity. The relative bulk density is calculated about 96.4% according to Archimedes principle. Moreover, the grains of the sample show quadrate-like morphology, different from that synthesized by conventional solid state reaction method in which the grains have an over much sintering. The average grain size of the sample is about 900 nm, which is much smaller than the $BiFeO_3$ bulk materials (3–5 μm) synthesized under normal pressure [8,18], implying that the rate of grain growth was suppressed under high pressure and low-sintering temperature.

Fig. 4(a) presents the field dependence of magnetization (M–H) curves for $BiFeO_3$ at 300 K. The enlarged part from −300 Oe to

Table 1
The refined crystal structure parameters of the high-pressure synthesized $BiFeO_3$ compound at room temperature.

Cell (Å)	Atoms	Position	*x*	*y*	*z*
$a = 5.5818(3)$	Bi	6a	0	0	0
$c = 13.8692(1)$	Fe	6a	0	0	0.2215(1)
$c = 374.22(4)$	O	18b	0.4406(0)	0.0011(9)	0.9563(3)
$R_{wp} = 8.1\%, R_p = 7.6\%$					

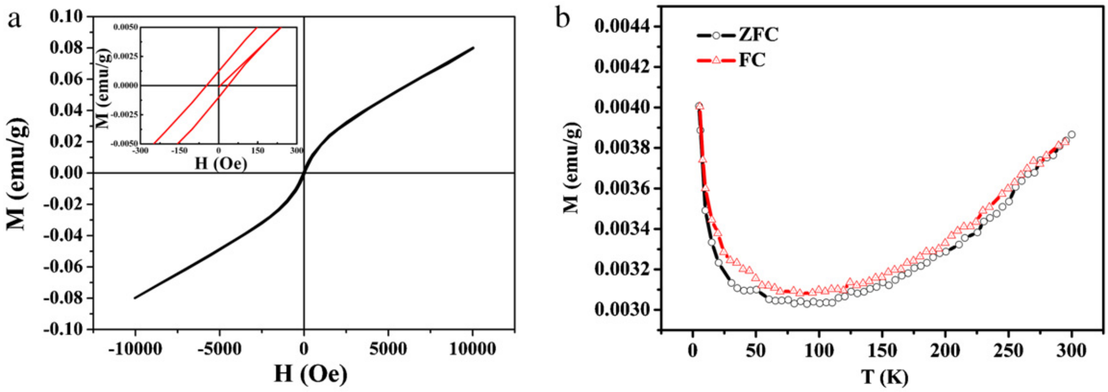

Fig. 4. (a) The field dependence of magnetization (M–H) curves for $BiFeO_3$. The inset shows the enlarged part from −300 Oe to 300 Oe. (b) ZFC and FC M–T under field of 1 kOe from 5 K to 300 K.

300 Oe is shown in the inset of Fig. 4(a). In contrast with the room-temperature linear field dependent magnetization for $BiFeO_3$ bulk materials synthesized under normal pressure [8,9], our sample exhibits a non-linear one. Su et al. [19] and Wen et al. [20] also found a similar behavior in their $BiFeO_3$ ceramics, which were synthesized by high-pressure annealing the so-gel-derived $BiFeO_3$ powders. Indeed, the observed shape of M–H loop and magnitude of the magnetization in the present work are very close to the $BiFeO_3$ nanocrystals with an average size of 40 nm reported by Mazumder et al. [21]. They argued that the enhancement of magnetization mainly comes from the incomplete spins along the direction of the wave vector, the emergence of Fe^{2+} and the lattice strain. In the present work, the modified Fe–O–Fe angle (158.4°) would destroy the spiral spin structure and lead to the net magnetization. The average grain size is about 900 nm, which is much larger than the spiral spin period of 62 nm. In addition, the above XPS analysis confirms that no Fe^{2+} exists in our sample. Therefore, it is suggested that the weak magnetism should be ascribed to the lattice distortion induced by the high-pressure annealing.

The zero field cooled (ZFC) and field cooled (FC) temperature dependent magnetization curves were measured under 1 kOe from 5 to 300 K, as shown in Fig. 4(b). Both the FC and ZFC curves drop slightly with decreasing temperature from 300 to 100 K, confirming the antiferromagnetic exchange interaction of spins. The fast

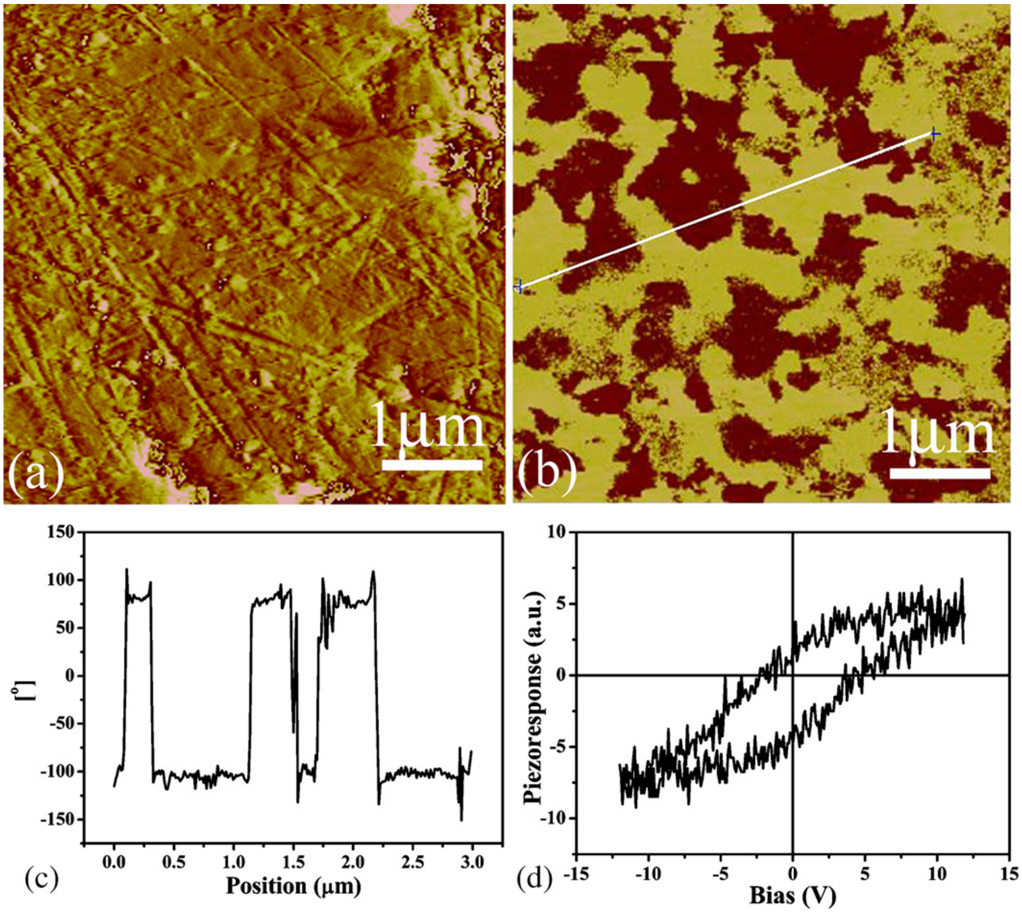

Fig. 5. (a) The topography and (b) piezoresponse images of $BiFeO_3$ compound. (c) Line-scanning piezoresponse signal. (d) Piezoresponse hysteresis loop of the sample.

increase of magnetization with decreasing temperature below 50 K was also observed, which was attributed to the development of incommensurate sinusoidal spin structure in $BiFeO_3$[22]. The magnetization value of FC curve measured under same magnetic field was slightly higher than that of ZFC curve, indicating the weak ferromagnetic properties. However, more detailed work is needed, such as neutron diffraction, to fully understand magnetic structure or spin configuration in high-pressure annealed $BiFeO_3$.

The ferroelectric behavior of the sample was investigated by piezoresponse force microscopy (PFM). The sample was fixed with silver paint acting as a bottom electrode while a bias is applied on the conductive atomic force microscope tip used as the top electrode. Imaging of the domains is carried out by applying a small ac bias on the bottom electrode giving rise to the converse piezoelectric effect detect through lock-in techniques [23]. Fig. 5(a) and (b) shows the topography and the corresponding piezoresponse images of polished $BiFeO_3$ compound, respectively. There are some scratches but no grains and boundaries can be seen on the surface (Fig. 5(a)) owing to the rigorous polishing process. The correlation between topography and piezoresponse is weak, indicating the little contribution of the electrostatic signal. The piezoelectric contrasts are clearly seen on the PFM image (Fig. 5(b)), which is similar to that of single crystal [24]. No regular domains like Ref. [25] were observed. This might be ascribed to the relatively rough surface of the sample. By scanning along the white line indicated in Fig. 5(b) we obtained Fig. 5(c). From Fig. 5(c), we can see that the piezoresponse signal shows antiparallel polar phase and the domain width is about several micrometers. The local hysteresis measurements were performed by keeping the tip fixed above the surface and applying dc voltage while recording the piezoresponse signal. A typical hysteresis loop was shown in Fig. 5(d), which unambiguously confirms the ferroelectric nature of the sample at room temperature.

4. Conclusion

High-density polycrystalline $BiFeO_3$ compound was successfully synthesized by high-pressure annealing method. The results of refinement show the sample possesses a distorted *R*3*c* structure. The SEM images demonstrate that high-pressure annealing can lower the grain growth rate and increased the density of the ceramic. Clear magnetic hysteresis loop with remnant magnetization has been observed in high-pressure synthesized $BiFeO_3$ at room temperature. Irregular domains were observed on the surface of the sample by piezoresponse force microscopy, and a typical hysteresis loop was obtained.

Acknowledgements

This work is supported by National Key Projects for Basic Research of China (Nos. 2005CB623605 and 2010CB923404).

References

[1] N.A. Spaldin, M. Fiebig, Science 309 (2005) 391.
[2] M. Fiebig, J. Phys. D: Appl. Phys. 38 (2005) R123.
[3] J.D. Bucci, B.K. Robertson, W.J. James, J. Appl. Crystallogr. 5 (1972) 187.
[4] J.M. Moreau, C. Michel, R. Gerson, W.J. James, J. Phys. Chem. Solids 32 (1971) 1315.
[5] C. Ederer, N.A. Spaldin, Phys. Rev. B 71 (2005) 224103.
[6] I. Sosnowska, T. Peterlin-Neumaier, E. Steichele, J. Phys. C: Solid State Phys. 15 (1982) 4835.
[7] G. Catalan, J.F. Scott, Adv. Mater. 21 (2009) 2463.
[8] M. Kumar, V. Palkar, K. Srinivas, S. Suryanarayana, Appl. Phys. Lett. 76 (2000) 2764.
[9] Y. Wang, L. Zhou, M. Zhang, X. Chen, J. Liu, Z. Liu, Appl. Phys. Lett. 84 (2004) 1731.
[10] S.T. Zhang, M.H. Lu, D. Wu, Y.F. Chen, N.B. Ming, Appl. Phys. Lett. 87 (2005) 262907.
[11] A.A. Belik, T. Yokosawa, K. Kimoto, Y. Matsui, E. Takayama-Muromachi, Chem. Mater. 19 (2007) 1679.
[12] A.A. Belik, S. Iikubo, K. Kodama, N. Igawa, S. Shamoto, E. Takayama-Muromachi, Chem. Mater. 20 (2008) 3765.
[13] A.A. Belik, T. Wuernisha, T. Kamiyama, K. Mori, M. Maie, T. Nagai, Y. Matsui, E. Takayama-Muromachi, Chem. Mater. 18 (2006) 133.
[14] Y.G. Shi, S.L. Tang, L.Y. Lv, J.Y. Fan, J. Alloys Compd. 506 (2010) 533.
[15] A. Larson, R. Von Dreele, Los Alamos National Laboratory Report LAUR, 2004.
[16] F. Kubel, H. Schmid, Acta Crystallogr. Sect. B 46 (1990) 698.
[17] P. Mills, J.L. Sullivan, J. Phys. D: Appl. Phys. 16 (1983) 723.
[18] A.K. Pradhan, K. Zhang, D. Hunter, J.B. Dadson, G.B. Loiutts, P. Bhattacharya, R. Katiyar, J. Zhang, D.J. Sellmyer, U.N. Roy, Y. Cui, A. Burger, J. Appl. Phys. 97 (2005) 093903.
[19] W.N. Su, D.H. Wang, Q.Q. Cao, Z.D. Han, J. Yin, J.R. Zhang, Y.W. Du, Appl. Phys. Lett. 91 (2007) 092905.
[20] F. Wen, N. Wang, F. Zhang, Solid State Commun. 150 (2010) 1888.
[21] R. Mazumder, P. Sujatha Devi, D. Bhattacharya, P. Choudhury, A. Sen, M. Raja, Appl. Phys. Lett. 91 (2007) 062510.
[22] V.B. Naik, R. Mahendiran, Solid State Commun. 149 (2009) 754.
[23] A. Kholkin, I. Bdikin, D. Kiselev, V. Shvartsman, S. Kim, J. Electroceram. 19 (2007) 81.
[24] D. Lebeugle, D. Colson, A. Forget, M. Viret, P. Bonville, J.F. Marucco, S. Fusil, Phys. Rev. B 76 (2007) 024116.
[25] V.V. Shvartsman, W. Kleemann, R. Haumont, J. Kreisel, Appl. Phys. Lett. 90 (2007) 172115.